Vanishing $N = 20$ Shell Gap: Study of Excited States in ^{27,28}Ne

Zs. Dombrádi,[1] Z. Elekes,[1,2] A. Saito,[3] N. Aoi,[2] H. Baba,[3] K. Demichi,[3] Zs. Fülöp,[1] J. Gibelin,[4] T. Gomi,[3] H. Hasegawa,[3]
N. Imai,[5] M. Ishihara,[2] H. Iwasaki,[5] S. Kanno,[3] S. Kawai,[3] T. Kishida,[2] T. Kubo,[2] K. Kurita,[3] Y. Matsuyama,[3]
S. Michimasa,[5] T. Minemura,[2] T. Motobayashi,[2] M. Notani,[5] T. Ohnishi,[5] H. J. Ong,[5] S. Ota,[6] A. Ozawa,[7] H. K. Sakai,[3]
H. Sakurai,[5] S. Shimoura,[5] E. Takeshita,[3] S. Takeuchi,[2] M. Tamaki,[5] Y. Togano,[3] K. Yamada,[3]
Y. Yanagisawa,[2] and K. Yoneda[2]

[1]*Institute of Nuclear Research of the Hungarian Academy of Sciences, P.O. Box 51, Debrecen, H-4001, Hungary*
[2]*The Institute of Physical and Chemical Research, 2-1 Hirosawa, Wako, Saitama 351-0198, Japan*
[3]*Rikkyo University, 3 Nishi-Ikebukuro, Toshima, Tokyo 171, Japan*
[4]*Institut de Physique Nucléaire, 15 rue Georges Clemenceau 91406 Orsay, France*
[5]*University of Tokyo, Tokyo 1130033, Japan*
[6]*Kyoto University, Kyoto 606-8501, Japan*
[7]*University of Tsukuba, Tennoudai 1-1-1, Tsukuba-shi, Ibaraki 305-8571, Japan*
(Received 13 July 2005; published 11 May 2006)

This Letter reports on the ^{1}H(^{28}Ne, ^{28}Ne) and ^{1}H(^{28}Ne, ^{27}Ne) reactions studied at intermediate energy using a liquid hydrogen target. From the cross section populating the first 2^+ excited state of ^{28}Ne, and using the previously determined $B(E2)$ value, the neutron quadrupole transition matrix element has been calculated to be $M_n = 13.8 \pm 3.7$ fm^2. In the neutron knockout reaction, two low-lying excited states were populated in ^{27}Ne. Only one of them can be interpreted by the sd shell model while the additional state may intrude from the fp shell. These experimental observations are consistent with the presence of fp shell configurations at low excitation energy in ^{27,28}Ne nuclei caused by a vanishing $N = 20$ shell gap at $Z = 10$.

The study of shell structure has played a crucial role in nuclear physics for a long time. The magic numbers 2, 8, 20, 28, 50, 82, and so on, associated with the shell closures in the atomic nucleus are well known close to the valley of stability. However, it is still a fundamental and presently open question whether the major shell closures and magic numbers change in very neutron-rich nuclei [1,2].

Experimental data accumulated since the late seventies on a missing $N = 20$ shell closure in the Mg-Na region launched the idea of the collapse of the usual shell model ordering of the single particle states in neutron-rich nuclei [3,4]. According to the early calculations, the effective single particle energy of the $f_{7/2}$ orbit becomes lower than that of the $d_{3/2}$ one in ^{28}O [4]. However, systematic investigations have revealed that the observed phenomena can also be described by considering a strong correlation energy associated with the proton-neutron $T = 0$ interaction leading to a large deformation [3,5] without assuming a significant change of the single particle energy structure. The deformed $2p$-$2h$ states may intrude below the normal spherical states and form an "island of inversion." In these calculations, the effective interaction, giving a reasonable description of nuclei close to the stability, leads to an effective $N = 20$ shell gap changing from 7 MeV at $Z = 20$ to about 5 MeV at $Z = 8$ [5,6]. This shell gap is in agreement with the value calculated with a mean field approximation [7], and large enough to conserve the spherical $N = 20$ shell closure. All the experimental data available around the "island of inversion" could be explained without the breakdown of the $N = 20$ shell closure [8].

As an alternative approach, the Monte Carlo diagonalization method has also been introduced in the shell model for the region of light neutron-rich nuclei adding the two lower fp shell orbits ($1f_{7/2}$ and $2p_{3/2}$) to the sd shell model space (Monte Carlo shell model—MCSM) [9]. The use of the enlarged valence space allows the mixing of the sd and fp configurations and gives a reasonable description of the available experimental data close to the "island of inversion" and even beyond [9–11]. However, its effective interaction leads to a rapid decrease of the shell gap to 1.2 MeV at $Z = 8$ [8] and raises the question again: does the $N = 20$ shell gap disappear at large neutron excess?

As a consequence of the rapidly decreasing shell gap, the MCSM predicts a much wider "island of inversion" than the models with a closed $N = 20$ shell. In this model, the crossing of the intruder and normal configurations takes place at $N = 18$ resulting in a deformed ground state even at this neutron number and low-energy intruder states up to $N = 17$. This difference encouraged the search for the border of the "island of inversion." Recently, the observation of two excited states at 1249 keV and 1588 keV in ^{29}Na [12] provided new data that support the MCSM prediction of having low-lying fp states mixed with the normal ones at $N = 18$ [12] and of a small $N = 20$ shell gap. On the other hand, a recent precise measurement of the $B(E2)$ value in ^{28}Ne [13] gives a value of 132(23) e^2 fm^4 that is much smaller than that of the MCSM calculation [9] (269 e^2 fm^4) and at a first glance seems to support the assumption of a small deformation. However, it is also

possible that the neutron deformation is large in ^{28}Ne, and the $0_1^+ \rightarrow 2_1^+$ transition is dominated by neutron excitation—as it was found for ^{16}C [14,15]—which could not be observed in the above experiment.

To determine what extent the intruder configurations from the fp shell disturb the structure of the neutron-rich Ne nuclei, we studied the ^{28}Ne nucleus via inelastic proton scattering which allows us to determine the deformation of the neutron distribution employing the existing data on $B(E2)$. In addition, we also investigated the excited states of ^{27}Ne simultaneously by neutron knockout reaction in order to contribute to the clarification of the question whether the $N = 20$ shell gap exists at small Z values.

The experiment was performed at the RIKEN Accelerator Research Facility. An ^{40}Ar primary beam of 94 MeV/nucleon energy with 60 pnA intensity was transported to a ^{181}Ta production target of 0.5 cm thickness. The RIKEN projectile fragment separator [16] analyzed the momentum and mass of the reaction products. An aluminum wedged degrader of 221 mg/cm^2 was put at the momentum dispersive focal plane (F1) for purifying the constituents. The secondary beam included neutron-rich O, F, Ne, and Na nuclei with $A/Z \approx 3$. The fragment separator was set to its full 6% momentum acceptance. The total intensity was about 100 particle/s (pps) while the ^{28}Ne intensity reached 20 pps on average. The identification of the incident beam species was performed on an event by event basis by means of energy loss, time-of-flight (TOF), and magnetic rigidity ($B\rho$) [17]. The separation of ^{28}Ne particles was complete. Two plastic scintillators of 1 mm thickness were placed at the first and second focal planes (F2 and F3) to measure the TOF. One silicon detector, with thickness of 0.35 mm, was inserted at F3 for energy loss determination. The secondary beam hit a liquid hydrogen target [18,19] of 30 mm diameter at F3. The thickness of the secondary target was 24 mm and its entrance and exit windows were made of 6.6 μm Aramid foil. The average areal density of the hydrogen was 210 mg/cm^2. The mean energy of ^{28}Ne isotopes in the target was calculated at 51.3 MeV/nucleon. Two parallel plate avalanche counters (PPACs) at F3 upstream of the target monitored the position of the incident particles. The beam spot size was 24 mm both in horizontal and vertical directions. The outgoing particles were detected and identified by a PPAC and a silicon telescope of three layers with thicknesses of 0.5 mm, 0.5 mm, and 1 mm located about 80 cm downstream of the target. Each layer was made of a 2×2 matrix of detectors, the active area of which was 48×48 mm^2. The Z identification was performed by TOF-energy loss method where the TOF was measured between the secondary target and the PPAC. The isotope separation was done by use of the $\Delta E - E$ method. The particle spectra are dominated by the beam particles; however, if we require coincidence with γ rays, the beam could be eliminated, making the $\Delta E - E$ method sensitive enough. It is demonstrated in Fig. 1 where the linearized mass
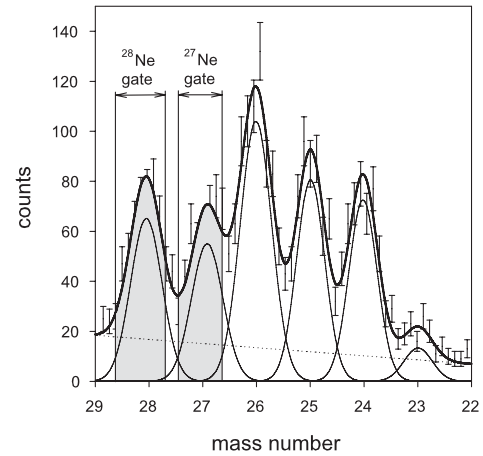

FIG. 1. Separation of neon isotopes using $\Delta E - E$ information in the silicon telescope. The bold solid line is a sum of 6 Gaussian functions and a polynomial background. The individual Gaussians and the background function are also plotted with thin solid lines.

spectrum of neon isotopes is shown for one segment of the 2×2 matrix Si telescope.

The deexcitation γ rays emitted by the inelastically scattered nuclei were detected by the DALI2 setup consisting of 146 NaI(Tl) scintillators [20] surrounding the target. The intrinsic energy resolution of the array was 10% (FWHM) for a 662 keV energy γ ray. In Fig. 2 the Doppler-corrected γ ray spectra for ^{28}Ne [Fig. 2(a)] and ^{27}Ne [Fig. 2(b)] nuclei are presented, which were produced by putting an additional gate on the time spectra of the NaI(Tl) detectors selecting the prompt events and subtracting the random coincidences.

By fitting the spectra with Gaussian functions and smooth exponential backgrounds, first, the positions of the peaks were determined to be 1319(22) keV and 1711(30) keV for ^{28}Ne and 765(20) keV and 904(21) keV for ^{27}Ne.

The energies for ^{28}Ne are in reasonable agreement with the values 1289(9) keV and 1719(11) keV measured earlier in Ref. [21] and 1320(20) keV in Ref. [22]. In Ref. [21] the 1711 keV transition is connected to the 1319 keV one establishing a state at 3030 keV. For ^{27}Ne, a 772(7) keV line was also observed in a fragmentation reaction [21] while a peak at 870(16) keV was recently detected in the ^{12}C(^{28}Ne, ^{27}Ne) reaction [13].

After the peak positions had been determined they were fed into the detector simulation software GEANT4 [23] and the resultant response curves plus smooth polynomial backgrounds were used to analyze the experimental spectra and obtain the cross sections in ^{28}Ne to be $\sigma(2_1^+ \rightarrow 0_1^+) = 32 \pm 4$ mb, $\sigma(X^+ \rightarrow 2_1^+) = 10 \pm 3$ mb (consequently with a feeding correction $\sigma(0_1^+ \rightarrow 2_1^+) = 22 \pm 5$ mb, $\sigma(0_1^+ \rightarrow X^+) = 10 \pm 3$ mb). From a distorted wave analysis of the cross sections, we derived the "matter" deformation length (δ_M). In the calculations, the standard collective form factors were applied and the global phe-
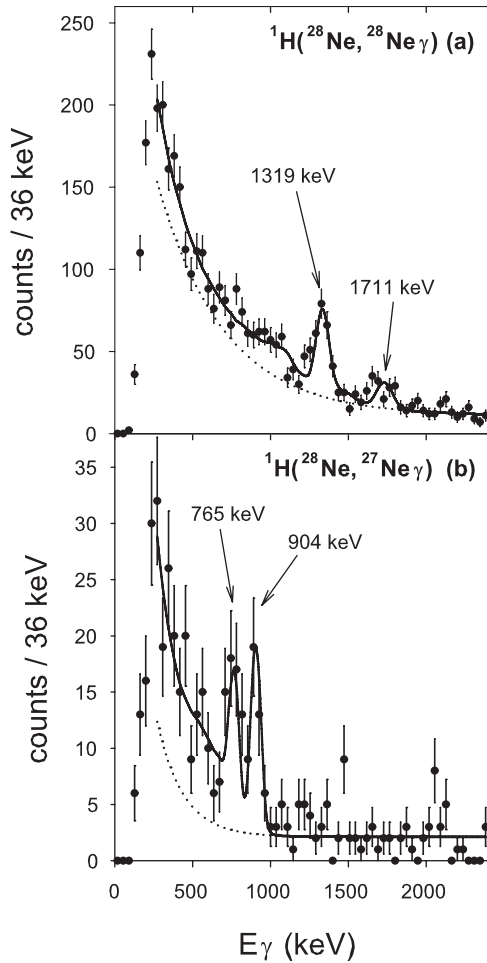
FIG. 2. Doppler-corrected spectra of γ rays emerging from ^{1}H(^{28}Ne, ^{28}Ne) (a) and ^{1}H(^{28}Ne, ^{27}Ne) (b) reactions. The solid line is the final fit including the spectrum curves from GEANT4 simulation and additional smooth polynomial backgrounds plotted as separate dotted lines for each nucleus.

nomenological parameter set CH89, proposed in [24], was employed for the optical potential. Beyond the statistical error, there might be an additional uncertainty caused by the choice of the optical potential parameter set. As was discussed in our earlier Letter [25], this involves 10%–20% error on the deformation parameters. The matter deformation length deduced in this way is $\delta_M = 0.95 \pm 0.18$ fm which corresponds to a moderate mass deformation of $\beta_M = 0.25 \pm 0.05$.

More detailed information on the structure of nuclei can be obtained by decomposing the mass transition probability into proton and neutron ones. For this purpose, we can apply the Bernstein formula [26], according to which

$$\frac{M_n}{M_p} = \frac{b_p}{b_n}\left[\frac{\delta_M}{\delta_C}\left(1 + \frac{b_n N}{b_p Z}\right) - 1\right]. \quad (1)$$

Here $bn/bp = 3$ are the sensitivity parameters for protons and neutrons of our (p, p') probe. Using the measured $B(E2)$ value [where the well-known formula

of $B(E2; 0_1^+ \rightarrow 2_1^+) = (\frac{3}{4\pi})^2 Z^2 R^2 \delta_C^2 e^2$ holds] of $132(23)$ e^2 fm^4 ($M_p = 11.5 \pm 1.0$ fm^2) [13] for ^{28}Ne, the ratio of neutron and proton multipole matrix elements can be calculated to be $M_n/M_p = 1.2 \pm 0.3$ corresponding to $M_n = 13.8 \pm 3.7$ fm^2. [It should be noted that the $B(E2)$ was determined earlier to be $269(136)$ e^2 fm^4 [22]. Since this result has a very large error of 50%, the data in Ref. [13] were used in the following.] The M_n/M_p ratio for ^{28}Ne is close to unity, which is quite far from the $N/Z = 1.8$ ratio, showing that the 2_1^+ excitation cannot be characterized by the coherent motion of protons and neutrons. With the relation $\delta_{n(p)} = R\beta_{n(p)}$, it is possible to deduce the neutron and proton deformation parameters. This results in $\beta_n = 0.23 \pm 0.05$ using the $\beta_p = 0.36 \pm 0.03$ value derived from the experimental $B(E2)$ [13]. Thus, both the neutron and the proton deformations are much smaller than is characteristic of nuclei in the "island of inversion" and means that also the concept on a strongly enhanced neutron transition probability that compensates the small $B(E2)$ can be rejected.

Although the experimental values of the $B(E2)$ and the neutron transition matrix element seem to support the persistence of the $N = 20$ shell closure, the picture with a vanishing shell gap [9] cannot be rejected, either. A reason for the failure of the MCSM in reproducing the present experimental result may be the overestimation of the effective charges in the theoretical calculation [9]. An isopin dependence of the effective charges was proposed by Bohr and Mottelson [27], the importance of which was recognized by Sagawa and Asahi [28] close to the neutron dripline. Indeed, a strong decrease of the neutron effective charge has been observed in nuclei far from the valley of stability like ^{16}C [14] or ^{17}B [25]. In Sagawa and Asahi's model, the effective charges are reduced to $e_n = 0.14$ and $e_p = 0.3$ [28] for ^{28}Ne.

With these values, both the $B(E2)$ and the neutron transition matrix elements can be described in a correct way in the MCSM [29], but the neutron transition probability becomes strongly underestimated in the sd shell model. Although the neutron transition probability measured in the present work clearly discriminates between the two approaches, to exploit this feature, the value of the effective charges should be fixed in the region.

The validity of the above models can be further checked by investigation of odd nuclei. Direct observation of a single particle state from the fp shell could pose a stringent test on the $N = 20$ shell gap. In the sd shell model, the number of predicted bound excited states is one in ^{27}Ne (i.e., $s_{1/2}$) while MCSM allows three of them (i.e., $s_{1/2}$, $p_{3/2}$, and $f_{7/2}$). The γ-ray spectrum of ^{27}Ne in Fig. 2 shows that two excited states at 765 keV and 904 keV are populated with similar intensities. (These two transitions cannot be coincident, since it would result in a state above the neutron separation energy ($S_n \sim 1400$ keV). Comparing our level scheme with the one calculated in the sd shell model shown in Fig. 3, it is seen that one of the excited

5/2+	2170		
7/2-	2017		
1/2+	868	(1/2+)	904
		(3/2-)	765
3/2+	0	(3/2+)	0
USD		EXP	

^{27}Ne

FIG. 3. Experimentally determined low-lying levels of ^{27}Ne nucleus plotted together with the predictions of shell model calculation using *USD* interaction [32].

states may correspond to the $1/2^+$ state predicted by both models; the other one should come from out of the *sd* shell model space excitation. Since it decays by a prompt transition to the presumed $3/2^+$ ground state, the additional excited state may correspond to the theoretical $3/2^-$ one of MCSM, associated with the $\nu p_{3/2}$ configuration. (The decay of the $7/2^-$ state predicted by the MCSM to the $3/2^+$ ground state cannot be visible in the present experiment due to its long lifetime even if it is bound.) Thus, the observation of two low-lying excited states in ^{27}Ne is in agreement with the MCSM prediction.

Having single particle states, and considering the pairing energy difference between the *s* and *d* orbits, the 3.8 MeV estimation of the MCSM for the $N = 16$ shell gap is consistent with our results. On the other hand, the $N = 20$ shell gap would be about 1 MeV. Since the low energy of the intruder configuration can be associated with proton-neutron quadrupole correlation, which results in a Nilsson-like orbit proposed by the MCSM calculation, from the energies obtained in the present work, we can consider the value deduced above only as a lower limit.

Although the observed small neutron transition probability in ^{28}Ne might be interpreted both in the pure *sd* shell model and MCSM, the detection of two low-lying excited states in ^{27}Ne together with the anomalies previously observed in the energies of the excited states along the $N = 18$ line, namely, the appearance of excited states around 1.5 MeV in ^{29}Na [12], the low energy of the 2^+ state in ^{28}Ne [22,30], and the presence of a low-energy state in ^{28}F [31] can be considered as a clear and consistent set of data indicating a small $N = 20$ shell gap.

Summarizing our results, we have studied the ^{28}Ne nucleus by $(p, p'\gamma)$ inelastic scattering in inverse kinematics. Using the recently measured $B(E2; 0_1^+ \rightarrow 2_1^+)$ value ($M_p = 11.5 \pm 1.0$ fm^2), the neutron transition matrix element $M_n = 13.8 \pm 3.7$ fm^2 was determined. These values are much smaller than is characteristic of nuclei in the "island of inversion" and mean that the concept on a

strongly enhanced neutron transition probability that compensates the small $B(E2)$ and explains the low energy of the 2_1^+ state cannot be valid. While the transition probabilities might be interpreted by both the calculations within the *sd* and *sdpf* shell models with appropriate parameters, the observation of two bound excited states in ^{27}Ne in the one-neutron-removal reaction supports a vanishing $N = 20$ shell gap.

Note added in proof.—Parallel to the present work, the 765 keV state in ^{27}Ne was assigned to a neutron *p* configuration from the ^{26}Ne(d, p) reaction [33].

[1] D. Warner, Nature (London) **430**, 517 (2004).
[2] J. Fridmann *et al.*, Nature (London) **435**, 922 (2005).
[3] B. Wildenthal *et al.*, Phys. Rev. C **22**, 2260 (1980).
[4] M. Storm *et al.*, J. Phys. G **9**, L165 (1983).
[5] E. Warburton *et al.*, Phys. Rev. C **41**, 1147 (1990).
[6] J. Retamosa *et al.*, Phys. Rev. C **55**, 1266 (1997).
[7] S. Peru *et al.*, Eur. Phys. J. A **9**, 35 (2000).
[8] E. Caurier *et al.*, Nucl. Phys. **A693**, 374 (2001).
[9] Y. Utsuno *et al.*, Phys. Rev. C **60**, 054315 (1999).
[10] Y. Utsuno *et al.*, Phys. Rev. C **70**, 044307 (2004).
[11] Y. Utsuno *et al.*, Phys. Rev. C **64**, 011301(R) (2001).
[12] V. Tripathi *et al.*, Phys. Rev. Lett. **94**, 162501 (2005).
[13] H. Iwasaki *et al.*, Phys. Lett. B **620**, 118 (2005).
[14] Z. Elekes *et al.*, Phys. Lett. B **586**, 34 (2004).
[15] H. Ong *et al.*, Phys. Rev. C (to be published).
[16] T. Kubo *et al.*, Nucl. Instrum. Methods Phys. Res., Sect. B **70**, 309 (1992).
[17] H. Sakurai *et al.*, Phys. Lett. B **448**, 180 (1999).
[18] H. Akiyoshi *et al.*, RIKEN Accelerator Progress Report **32**, 167 (1998).
[19] H. Ryuto *et al.*, Nucl. Instrum. Methods Phys. Res., Sect. A **555**, 1 (2005).
[20] S. Takeuchi *et al.*, RIKEN Accelerator Progress Report **36**, 148 (2003).
[21] M. Belleguic *et al.*, Phys. Rev. C **72**, 054316 (2005).
[22] B. Pritychenko *et al.*, Phys. Lett. B **461**, 322 (1999).
[23] S. Agostinelli *et al.*, Nucl. Instrum. Methods Phys. Res., Sect. A **506**, 250 (2003).
[24] R. Varner *et al.*, Phys. Rep. **201**, 57 (1991).
[25] Z. Dombrádi *et al.*, Phys. Lett. B **621**, 81 (2005).
[26] A. Bernstein *et al.*, Phys. Rev. Lett. **42**, 425 (1979).
[27] A. Bohr *et al.*, *Nuclear Structure* (World Scientific, Singapore, 1998), Vol. II.
[28] H. Sagawa *et al.*, Phys. Rev. C **63**, 064310 (2001).
[29] T. Otsuka (private communication) based on Phys. Rev. C **60**, 054315 (1999).
[30] F. Azaiez *et al.*, AIP Conf. Proc. **495**, 171 (1990).
[31] Z. Elekes *et al.*, Phys. Lett. B **599**, 17 (2004).
[32] B. Brown, www.nscl.msu.edu/ brown/resources/ SDE.HTM.
[33] A. Obertelli *et al.*, Phys. Lett. B **633**, 33 (2006).